

## CO<sub>2</sub> Activation by Nb<sup>+</sup> and NbO<sup>+</sup> in the Gas Phase. A Case of Two-State Reactivity Process<sup>†</sup>

S. Di Tommaso, T. Marino, F. Rondinelli, N. Russo, and M. Toscano\*

*Dipartimento di Chimica and Centro di Calcolo ad Alte Prestazioni per Elaborazioni Parallele e Distribuite—Centro d'Eccellenza MIUR, Universita' della Calabria, I-87030 Arcavacata di Rende (CS), Italy*

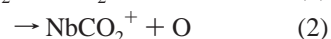
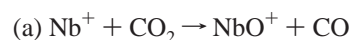
Received January 13, 2007

**Abstract:** Gas-phase carbon dioxide activation by Nb<sup>+</sup> and NbO<sup>+</sup> was studied at the density functional level of theory using the hybrid exchange correlation functional B3LYP. Three reaction profiles corresponding to the quintet, triplet, and singlet multiplicities were investigated in order to ascertain the presence of some spin inversion during the CO<sub>2</sub> reduction. Carbon dioxide activation mediated by metal cations was found to be an exothermic spin-forbidden process resulting from a crossing between quintet and triplet energetic profiles. The endothermic reaction of NbO<sup>+</sup> with carbon dioxide was a barrierless process involving spin inversion. Geometries of minima along potential energy surfaces and reaction heats were in agreement with those from experimental studies carried out by using a guided ion beam tandem mass spectrometer.

### 1. Introduction

The possibility of activating carbon dioxide, the main greenhouse gas, has received considerable attention in previous years.<sup>1–5</sup> As it is not possible to reduce significantly CO<sub>2</sub> emissions from anthropic sources, the interest in its chemical fixation<sup>6</sup> and utilization as a starting material of chemically useful compounds is increased. However, only nature can effectively regenerate organic molecules from carbon dioxide by using it as a one-carbon building block.<sup>7</sup> In previous years, chemical processes based on the use of metal species as catalysts for carbon dioxide reduction were investigated, both experimentally and theoretically.<sup>8–11</sup> By using a guided ion beam mass spectrometer, Sievers and Armentrout elucidated the reaction mechanisms of bare zirconium<sup>12</sup> and niobium<sup>13</sup> cations and those of their respective monoxide and dioxide cations with CO<sub>2</sub>. Details of the zirconium-ion-assisted CO<sub>2</sub> reduction potential energy surface were obtained by density functional theory.<sup>14</sup> Experimental data highlight the importance of analyzing the electronic terms and symmetry of metal cations involved in ground and excited states' energetic profiles. In this paper,

we studied, at the same level of theory used for the activation of carbon dioxide by zirconium,<sup>12</sup> the following reactions:



Our main aim was to elucidate the reaction mechanisms and determine the activation barriers useful to give insight into kinetic aspects. In particular, analysis of potential energy surfaces (PES), vibrational characterization of stationary and saddle points of each reaction pathway, and determination of exothermicity and endothermicity and bond dissociation energies were carried out in our work.

### 2. Computational Methods

All calculations were performed using the Gaussian 03 package.<sup>15</sup> Full optimizations were carried out for all molecular structures involved in the reaction mechanisms by means of B3LYP/DFT methods<sup>16,17</sup> in connection with the 6-311+G\*\* basis set<sup>18,19</sup> for nonmetal atoms and the LANL2DZ pseudopotential<sup>20</sup> for niobium ions. Energetic values include zero-point energy corrections obtained from the vibrational analysis.

<sup>†</sup> Dedicated to Professor Dennis R. Salahub on the occasion of his 60th birthday.

\* Corresponding author fax: +39-0984-493390; email: m.toscano@unical.it.

Transition states were confirmed applying the intrinsic reaction-coordinated procedure implemented in the Gaussian 03 package.<sup>21,22</sup>

The most stable electronic states of bare niobium and metal monoxide and dioxide monocations as well as those of all other species were carefully searched by the Alter keyword that ensures that the orbitals selected for occupation in the wavefunction are those of lowest energy. Wave function stability was tested by the Stable calculation method.<sup>23–25</sup>

### 3. Results and Discussion

#### 3.1. Determination of Metal Species Electronic States.

If a reaction profile involves crossings of different spin surfaces along the reaction coordinate, then it is described as a two-state reactivity pathway.<sup>26</sup> Such a type of mechanism requires the determination of the correct reactivity scale for metal cations' ground and excited states, or in other words the exactness of electronic states' ordering and splitting. According to our calculations, the electronic configuration of the Nb<sup>+</sup> ground state (<sup>5</sup>D) was found to be 4d<sup>4</sup>, while among its excited states, <sup>3</sup>P was the lowest in energy with a 4d<sup>4</sup> configuration too. The energy gap between the ground and first excited states was evaluated to be 17.25 kcal/mol, in good agreement with the experimental energy separation of 15.91 kcal/mol reported by Sievers and Armentrout.<sup>13</sup>

Nb<sup>+</sup> in its lowest singlet state (<sup>1</sup>S with configuration 4d<sup>4</sup>) lies at 23.72 kcal/mol above the <sup>5</sup>D quintet.

Photoelectronic studies carried out by Dyke and co-workers<sup>27</sup> by ionizing the NbO molecule in its ground state (<sup>4</sup>Σ<sup>−</sup>) hypothesized <sup>3</sup>Σ<sup>−</sup> as the ground state of the NbO<sup>+</sup> cation.

Our computations confirmed this suggestion deriving from a 2σ<sup>2</sup>1π<sup>4</sup>1δ<sup>2</sup> electronic configuration.

NbO<sup>+</sup> singlet (<sup>1</sup>A') and quintet (<sup>5</sup>Σ<sub>u</sub>) excited electronic states were found to lie at 4.84 and 53.04 kcal/mol above the ground state, respectively.

Neither experimental nor theoretical information exists for the NbO<sub>2</sub><sup>+</sup> ground state. Our B3LYP study indicated that the lowest-energy configuration of the niobium dioxide monocation has the singlet multiplicity (<sup>1</sup>A<sub>1</sub>) like its isovalent ZrO<sub>2</sub> neutral molecule.<sup>13,28</sup> Triplet (<sup>3</sup>B<sub>2</sub>) and quintet (<sup>5</sup>B<sub>2</sub>) excited states were found at 1.7 and 5.15 eV above the ground state, respectively.

On the basis of these results, it appears clear that the processes (a and b) to be investigated are, in principle, spin-forbidden reactions. Furthermore, the participation of the highest excited states is very unlikely; thus, the energetic profile for these multiplicities was not reported. However, energetic data were included in the tables.

**3.2. Path a: Activation of CO<sub>2</sub> by Nb<sup>+</sup>.** The most stable structure of the first adduct along the potential energy profile concerning path a (see Figure 1) was obtained by considering all known different coordination modes ( $\eta_o^1$ ,  $\eta_{o,o}^2$ ,  $\eta_{c,o}^2$ , and  $\eta_c^1$ ) of CO<sub>2</sub> to a transition metal atom.<sup>29</sup> Full optimizations of these starting geometries did not always give stable molecular systems as the data of Table 1 demonstrate. In particular, we have observed that the  $\eta_{c,o}^2$  structure in its quintet spin state collapsed in  $\eta_o^1$ , while singlet  $\eta_c^1$  evolved in  $\eta_{c,o}^2$ . The triplet  $\eta_{c,o}^2$ , singlet  $\eta_{o,o}^2$ , and quintet  $\eta_c^1$

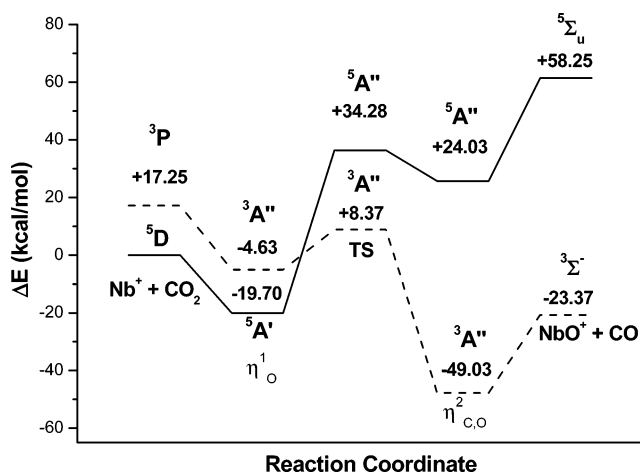


**Figure 1.** Potential energy surfaces relating to the Nb<sup>+</sup> + CO<sub>2</sub> reaction for quintet and triplet spin states.

**Table 1.** Absolute (*E* in au) Energies for Different NbCO<sub>2</sub><sup>+</sup> Isomers

coordination modes	quintet	triplet	singlet
	<i>E</i>	<i>E</i>	<i>E</i>
$\eta_o^1$	−244.576 973	−244.552 958	244.541 046
$\eta_{o,o}^2$	−244.521 936	−244.521 655	no coordination
$\eta_{c,o}^2$	in $\eta_o^1$	no coordination	−244.527461
$\eta_c^1$	no coordination	−244.515227	in $\eta_{c,o}^2$

optimizations led to weak adducts in which CO<sub>2</sub> was practically not coordinated to the cation.

For all examined multiplicities, the most stable coordination of niobium to carbon dioxide was found to be the  $\eta_o^1$  one. Quintet  $\eta_o^1$  constitutes the deepest minimum lying at 19.70 kcal/mol below the reactants asymptote. Irrespective of multiplicity, the  $\eta_o^1$  compounds always present a linear structure (see Figure 2) with similar geometrical parameters except for the Nb<sup>+</sup>–O bond length.

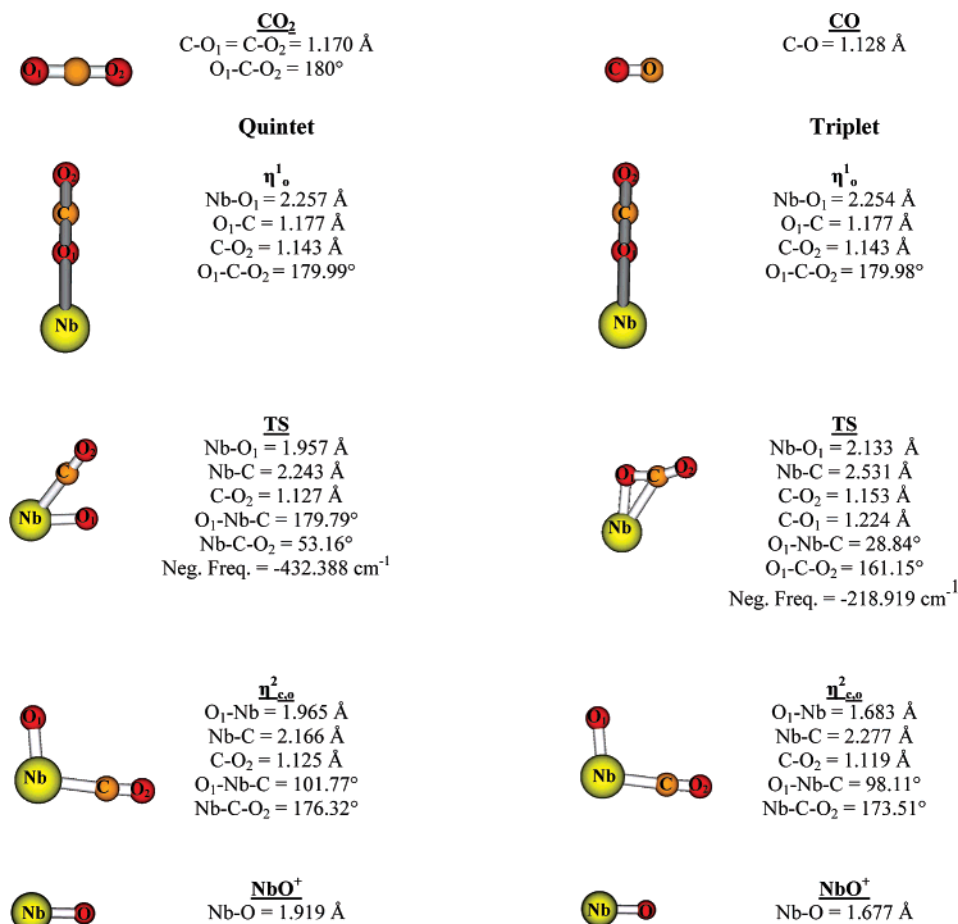
Absolute and relative energies for compounds lying on the path a PES are listed in Table 2.

For both spin states, the first step consists in the evolution of the  $\eta_o^1$  adduct in the  $\eta_{c,o}^2$  complex through a transition state (TS).

The three-center transition state on the quintet PES (<sup>5</sup>A'') lies at 34.28 kcal/mol above the energetic zero and is characterized by an imaginary vibrational frequency of 432 cm<sup>−1</sup> that corresponds to the stretching of the incoming Nb<sup>+</sup>–C bond coupled with the bending of the C–Nb<sup>+</sup>–O<sub>1</sub> angle.

The analogous transition state on the triplet surface (<sup>3</sup>A'') is located at 8.36 kcal/mol above the reactants asymptote in their electronic state of quintet. The imaginary frequency of 218 cm<sup>−1</sup> appears to be associated only with the bending of Nb<sup>+</sup>–O<sub>1</sub>–C because the Nb<sup>+</sup>–C distance is too long to observe its stretching in the computed IR spectrum.

From a structural point of view, the two transition states are quite different, as can be argued from parameters reported in Figure 2. A crossing between the two potential energy profiles suggests that a spin inversion occurs; thus, after the formation of the  $\eta_o^1$  molecular complex, the triplet multiplicity path becomes energetically favored.

**Figure 2.** Optimized structures and geometrical parameters of compounds relating to path a.**Table 2.** Absolute (*E* in au) and Relative ( $\Delta E$  in kcal/mol) Energies for the Compounds Having Quintet, Triplet, and Singlet Multiplicities Involved in Path a<sup>a</sup>

species	quintet		triplet		singlet	
	<i>E</i>	$\Delta E$	<i>E</i>	$\Delta E$	<i>E</i>	$\Delta E$
Nb <sup>+</sup> + CO <sub>2</sub>	-244.545 584	0	-244.518 091	17.25	-244.507 775	23.72
$\eta_o^1$	-244.576 973	-19.70	-244.552 958	-4.63	-244.541 046	2.85
TS	-244.490 952	34.28	-244.532 249	8.37	-244.524 269	13.36
$\eta_{c,o}^2$	-244.507 294	24.03	-244.623 721	-49.03	-244.617 693	-45.25
NbO <sup>+</sup> + CO	-244.452 742	58.25	-244.582 829	-23.37	-244.573 845	-17.73

<sup>a</sup>  $\Delta E$  values of excited states are referred to reactants' energy in their state of quintet.**Table 3.** Absolute (*E* in au) and Relative ( $\Delta E$  in kcal/mol) Energies for the Compounds Having Quintet, Triplet, and Singlet Multiplicities Involved in Paths b.1 and b.2

species	quintet		triplet		singlet	
	<i>E</i>	$\Delta E$	<i>E</i>	$\Delta E$	<i>E</i>	$\Delta E$
NbO <sup>+</sup> + CO <sub>2</sub>	-319.743 959	81.62	-319.874 046	0	-319.865 062	5.64
ONbCO <sub>2</sub> <sup>+</sup>	-319.784 405	56.25	-319.907 404	-20.93	-319.897 074	-14.45
NbO <sub>2</sub> <sup>+</sup> + CO	-319.633 760	150.77	-319.783 502	+56.81	-319.857 197	10.57
NbCO <sub>2</sub> <sup>+</sup> + O	-319.597 173	182.29	-319.713 600	+100.67	-319.707 572	104.46

In fact, travelling on the quintet PES, after TS, we found that the O-Nb<sup>+</sup>-CO  $\eta_{c,o}^2$  species is quite unstable (24.03 kcal/mol above reactants) and practically unreachable because of the presence of an activation barrier of about 54 kcal/mol.

Consequently, the NbO<sup>+</sup> and CO products, placed 58.25 kcal/mol above the reactants asymptote, cannot be obtained through this reaction channel.

Different features can be recognized in triplet energy surface. If we take into account the two-state reactivity

phenomenon, the second molecular intermediate  $\eta_{c,o}^2$  (<sup>3</sup>A'') is formed starting from the quintet  $\eta_o^1$  by overcoming an activation barrier of 28.06 kcal/mol. The  $\eta_{c,o}^2$  (<sup>3</sup>A'') species lies at 49.03 kcal/mol below the quintet reactants asymptote, while the products are placed at -23.37 kcal/mol on the PES.

If the overlap of potential energy surfaces is considered, the reduction of CO<sub>2</sub> by Nb<sup>+</sup> appears to be an exothermic process with a reaction heat of 23.37 kcal/mol and a rate-determining step that implies the clearing of an activation barrier of 28.06 kcal/mol. Furthermore, according to the spin

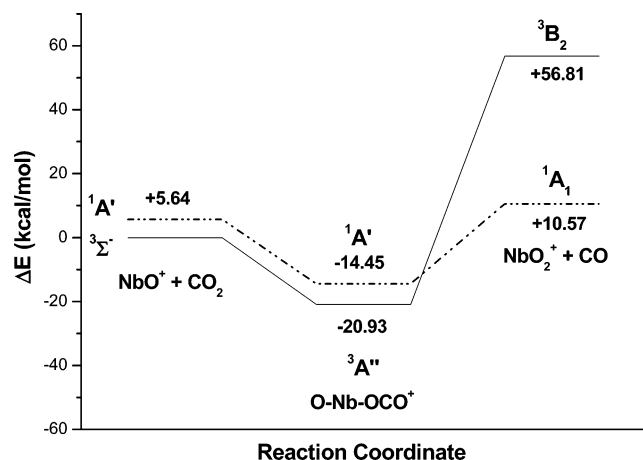


**Figure 3.** Energetic profiles relating to the interaction between  $\text{NbO}^+$  and  $\text{CO}_2$ : path b.1.

inversion occurrence, the overall mechanism is that of a spin-forbidden two-state reaction.

**3.3. Path b: Activation of  $\text{CO}_2$  by  $\text{NbO}^+$ .** Experimental data achieved by Sievers and Armentrout<sup>13</sup> suggest that  $\text{NbO}^+$  produced by path a, as elucidated above, reacts with carbon dioxide, giving rise to  $\text{NbO}_2^+ + \text{CO}$  or  $\text{NbCO}_2^+ + \text{O}$  products through two different channels of path b that we named b.1 and b.2.

Molecular structures involved in both these channels were optimized by considering quintet, singlet, and triplet spin states. As shown in Table 3, quintet stationary points have higher energy than the corresponding species with different multiplicities; thus, the relative PES was not further considered. Furthermore, it is also possible to note that irrespective of the considered multiplicity the formation of  $\text{NbCO}_2^+$  and atomic oxygen requires a huge quantity of energy, making meaningless the discussion about the b.2 path. However, it is worthwhile that both b.1 and b.2 profiles proceed through

a barrierless mechanism since the molecular adduct resulting from the interaction between  $\text{NbO}^+$  and  $\text{CO}_2$  evolves into the products without involving any transient structure. Besides, both b.1 and b.2 reaction paths are endothermic processes, as highlighted from relative energies listed in Table 3.

The triplet and singlet b.1 paths for the formation of  $\text{NbO}_2^+ + \text{CO}$  were reported in Figure 3. Optimized structures and geometrical parameters of species involved are shown in Figure 4.

The molecular adduct  $\text{O-Nb}^+-\text{OCO}$  with a triplet spin state is 20.93 kcal/mol more stable than the reactants, while products with the same multiplicity are located at very high energy (56.81 kcal/mol above the  $\text{NbO}^+$  and  $\text{CO}_2$  asymptote). The triplet pathway is therefore very endergonic.

On the contrary, on the singlet PES, the species  $\text{O-Nb}^+-\text{OCO}$  and the final products lie 14.45 and 10.57 kcal/mol below and above the reference, respectively.

A look to both potential energy surfaces shows that the formation of  $\text{NbO}_2^+ + \text{CO}$  is characterized by a spin inversion. The crossing occurs after the molecular adduct and entails that the reaction be a spin-forbidden process with reactants having a triplet multiplicity and products in the singlet spin state. The global process is endothermic for 10.57 kcal/mol.

## 4. Conclusions

Gas-phase interactions of  $\text{Nb}^+$  and  $\text{NbO}^+$  with carbon dioxide were examined at the density functional level of theory, by using B3LYP/6-311+G\*\*/LANL2DZ theoretical protocol. Triplet, quintet, and singlet multiplicities were analyzed for both pathways and for different reaction channels.

The singlet energy surface for the interaction of  $\text{Nb}^+$  with  $\text{CO}_2$  was found to be greatly disfavored because of the high energy of all stationary points. Between triplet and quintet

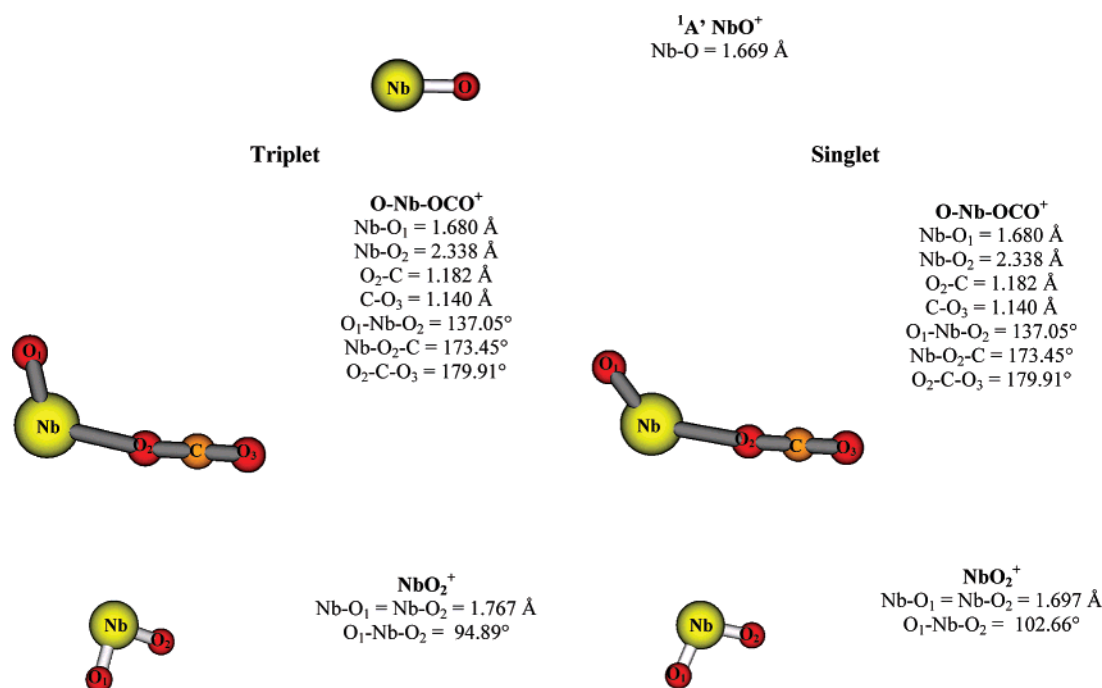


**Figure 4.** Optimized structures and geometrical parameters of compounds involved in path b.1.



potential energy profiles, a crossing occurs that causes a spin inversion at the transition-state level. Thus, CO<sub>2</sub> activation catalyzed by Nb<sup>+</sup> can be described as a two-state-reactivity process with a reaction heat of 23.37 kcal/mol.

In brief, the coordination of the niobium cation in its quintet ground state to CO<sub>2</sub> gives rise to the linear <sup>5</sup>A'  $\eta_o^1$  adduct that, through a transition state having triplet multiplicity, evolves in the <sup>3</sup>A''  $\eta_{c,o}^2$  compound, which in turn dissociates into the <sup>3</sup> $\Sigma^-$  NbO<sup>+</sup> and CO products.

The spin-forbidden profile is in agreement with the information derived by Sievers and Armentrout's mass spectrometry measurements.

The analysis of both possible reaction paths relating to NbO<sup>+</sup> and CO<sub>2</sub> interaction indicates that the most favored channel involves the abstraction of carbon dioxide oxygen by a monoxide cation.

The quintet potential energy profile as well as the path concerning the formation of NbCO<sub>2</sub><sup>+</sup> and O products are energetically unlikely.

The global reaction path for the formation of NbO<sub>2</sub><sup>+</sup> and CO derives from the overlap of triplet and singlet profiles showing a crossing following the formation of the ONb-OCO<sup>+</sup> molecular adduct, which causes a spin inversion. No transition state was observed for this process.

In our work, particular attention has received the determination of the electronic terms for metal compounds involved in all of the pathways, as some of them are unknown theoretically or experimentally. For the niobium cation, the comparison of our data with experimental ones indicates that the used level of theory is suitable enough to predict the exact ordering of triplet and quintet states other than the energetic gap between them.

**Acknowledgment.** We gratefully acknowledge the Dipartimento di Chimica, Università della Calabria for financial aid.

## References

- (1) Behr, A. *Carbon Dioxide Activation by Metal Complexes*; VCH: New York, 1998.
- (2) Louie, J.; Gibby, J. E.; Farnworth, M. V.; Tekavec, T. N. *J. Am. Chem. Soc.* **2002**, *124*, 15188.
- (3) Gibson, D. H. *Chem. Rev.* **1996**, *96*, 651.
- (4) Niemelä, M.; Nokkosmäki, M. *Catal. Today* **2005**, *100*, 269.
- (5) Solymosi, F. J. *J. Mol. Catal.* **1991**, *65*, 337.
- (6) Lu, X. B.; Wang, Y. *Angew. Chem., Int. Ed.* **2004**, *43*, 3574.
- (7) Brändén, C. I.; Schneider, G. *Carbon Dioxide Fixation and Reduction in Biological and Model Systems*; Oxford University Press: New York, 1994.
- (8) Avila, Y.; Barrault, J.; Pronier, S.; Kappenstein, C. *Appl. Catal., A* **1995**, *132*, 97.
- (9) Fujita, T.; Nishiyama, Y.; Ohtsuka, Y.; Asami, K.; Kusakabe, K. I. *Appl. Catal., A* **1995**, *126*, 245.
- (10) Otorbaev, D. K. *Chem. Phys.* **1995**, *196*, 543.
- (11) Sahibzada, M.; Chadwick, D.; Metcalfe, I. S. *Catal. Today* **1996**, *29*, 367.
- (12) Sievers, M. R.; Armentrout, P. B. *Int. J. Mass Spectrom.* **1999**, *185*, 117.
- (13) Sievers, M. R.; Armentrout, P. B. *Int. J. Mass Spectrom.* **1998**, *179*, 115.
- (14) Rondinelli, F.; Russo, N.; Toscano, M. *Theor. Chem. Acc.* **2006**, *115*, 434.
- (15) Frisch, M. J.; Trucks, G. W.; Schlegel, H. B.; Scuseria, G. E.; Robb, M. A.; Cheeseman, J. R.; Montgomery, J. A., Jr.; Vreven, T.; Kudin, K. N.; Burant, J. C.; Millam, J. M.; Iyengar, S. S.; Tomasi, J.; Barone, V.; Mennucci, B.; Cossi, M.; Scalmani, G.; Rega, N.; Petersson, G. A.; Nakatsuji, H.; Hada, M.; Ehara, M.; Toyota, K.; Fukuda, R.; Hasegawa, J.; Ispida, M.; Nakajima, T.; Honda, Y.; Kitao, O.; Nakai, H.; Klene, M.; Li, X.; Knox, J. E.; Hratchian, H. P.; Cross, J. B.; Adamo, C.; Jaramillo, J.; Gomperts, R.; Stratmann, R. E.; Yazyev, O.; Austin, A. J.; Cammi, R.; Pomelli, C.; Ochterski, J. W.; Ayala, P. Y.; Morokuma, K.; Voth, G. A.; Salvador, P.; Dannenberg, J. J.; Zakrzewski, V. G.; Dapprich, S.; Daniels, A. D.; Strani, M. C.; Farkas, O.; Malick, D. K.; Rabuck, A. D.; Raghavachari, K.; Foresman, J. B.; Ortiz, J. V.; Cui, Q.; Baboul, A. G.; Clifford, S.; Cioslowski, J.; Stefanov, B. B.; Liu, G.; Liashenko, A.; Piskorz, P.; Komaromi, V.; Martin, R. L.; Fox, D. J.; Keith, T.; Al-Laham, M. A.; Peng, C. Y.; Nanayakkara, A.; Challacombe, M.; Gill, P. M. W.; Johnson, B.; Chen, W.; Wong, M. W.; Gonzalez, C.; Pople, J. A. *Gaussian 03*; Gaussian, Inc: Wallingford, CT, 2004.
- (16) Lee, C.; Yang, W.; Parr, R. G. *Phys. Rev. B: Condens. Matter Mater. Phys.* **1998**, *37*, 785.
- (17) Colle, R.; Solvetti, D. *Theor. Chim. Acta* **1975**, *37*, 329.
- (18) McLean, A. D.; Chandler, G. S. *J. Chem. Phys.* **1980**, *72*, 5639.
- (19) Krishnan, R.; Binkley, J. S.; Seeger, R.; Pople, J. A. *J. Chem. Phys.* **1980**, *72*, 650.
- (20) Hay, P. J.; Wadt, W. R. *J. Chem. Phys.* **1985**, *82*, 284.
- (21) Gonzalez, C.; Schlegel, H. B. *J. Chem. Phys.* **1989**, *90*, 2154.
- (22) Gonzalez, C.; Schlegel, H. B. *J. Phys. Chem.* **1990**, *94*, 5523.
- (23) Seeger, R.; Pople, J. A. *J. Chem. Phys.* **1977**, *66*, 3045.
- (24) Bauernschmitt, R.; Ahlrichs, R. *J. Chem. Phys.* **1996**, *104*, 9047.
- (25) Schlegel, H. B.; Mc Douall, J. J. *Computational Advances in Organic Chemistry*; Ogretir, C., Csizmadia, J. G., Eds.; Kluwer Academic: The Netherlands, 1991.
- (26) Schröder, D.; Shaik, S.; Schwarz, H. *Acc. Chem. Res.* **2000**, *33*, 139.
- (27) Dyke, J. M.; Ellis, A. M.; Fehér, M.; Morris, A.; Paul, A. J.; Stevens, J. C. H. *J. Chem. Soc., Faraday Trans.* **1987**, *283*, 1555.
- (28) Siegbahn, P. E. M. *J. Phys. Chem.* **1993**, *97*, 9096.
- (29) Schaftenaar, G.; Noordik, J. H. *J. Comput.-Aided Mol. Des.* **2000**, *14*, 123.

CT700014K